

Fault diagnosis of power electronic circuits using optimized BP neural networks

Deye Jiang^{1*}, Shuting Huang^{1*}, and Juan Guo¹

¹School of Electronic Information, Guilin University of Electronic Technology, Beihai, 536000, China

Abstract. You should leave 8 mm of space above the abstract and 10 mm after the abstract. The heading Abstract should be typed in bold 9-point Arial. The body of the abstract should be typed in normal 9-point Times in a single paragraph, immediately following the heading. The text should be set to 1 line spacing. The abstract should be centred across the page, indented 17 mm from the left and right page margins and justified. It should not normally exceed 200 words. Three-phase rectifiers have a wide range of applications in industrial production and daily life, and failure to diagnose their faults promptly may affect the reliability of the system operation, resulting in huge safety hazards and economic losses. Therefore, it is of great significance to conduct online fault diagnosis research on the power electronic circuits within three-phase rectifiers. An optimized BP neural network algorithm is proposed for diagnosing open-circuit faults of thyristors in three-phase rectifier circuits. The output voltage waveform characteristics of the circuit, when a fault occurs, are analyzed, and the corresponding output voltage peaks at the same cycle time when different tubes are damaged under the fifth fault type are used as fault feature vectors, and the fault information is input into the BP, optimized BP neural network for training, and the trained neural network is used for fault diagnosis. The fault diagnosis accuracy was obtained by comparing the network output with the desired output. The results of simulation experiments show that the optimized BP neural network can diagnose and analyze the faults of rectifier circuits more efficiently than directly applying the BP network for fault diagnosis.

1 Introduction

Power electronics are devices used for the transformation of electrical energy and have a very wide range of applications in industry, electrical transport, and switching power supplies [1]. Rectifiers are key converters in power electronics. When it fails, it may cause damage to equipment and even loss of public property and life, therefore, fault detection of rectifiers is extremely important [2]. It is reported that more than 1/3 of rectifier failures are caused by circuit switching faults [3], and the performance and indicators of the switching components directly affect the whole circuit. Therefore, to improve the stability of the operation of power electronics, it is necessary to perform a fault diagnosis analysis of the switching devices of rectifiers. The switch devices in rectifier circuits often work at high voltages and high currents [4], which are characterized by high operating frequencies and high losses. If the heat is not dissipated in time, it is easy to cause damage to the devices, which will not only lead to an increase in output voltage ripple but also make the circuit work in an abnormal state. In actual operation, open circuits and short circuits of thyristors are common faults in rectifier circuits [5]. Generally, the number of thyristors in a rectifier circuit is large and it is difficult to quickly and accurately locate which thyristor is faulty. The traditional method of fault finding is used manually,

which is carried out using a case-by-case diagnosis. Due to the lack of detailed fault status information, it is not able to meet the needs of real-time diagnosis. With the development of intelligent technology, a technique that combines artificial intelligence and fault diagnosis has been proposed and has attracted extensive attention from many researchers and engineers. In [6], a data-driven approach is proposed for the online diagnosis of faults in single-phase PWM rectifiers. The method uses a nonlinear autoregressive exogenous (NARX) model and an extreme learning machine (ELM) to construct a signal predictor. During the diagnosis process, the predictor and the sensor run simultaneously, from which the residuals between them are obtained, and then the residuals are compared with the fault threshold, and the fault classification is completed by a classifier. The experimental results show that the method has a fast fault detection speed, high classification accuracy, and a certain level of robustness. In [7], a 12-pulse method for thyristor rectifier fault detection is proposed. The method uses a simple transformer that starts an alarm when a fault occurs and extracts a signal for one cycle, which allows a small amount of calculation to detect an open circuit fault in a three-phase SCR. In [8], a machine-learning algorithm is proposed for open-circuit fault detection in converters. The harmonic components are first analyzed to extract fault feature values, then the feature values are classified and input into a support

* Corresponding author: Shuting Huang, email: 313601037@qq.com

vector machine model, and finally, the trained model is applied to a microcontroller for testing. The experimental results show that the method effectively improves the accuracy and efficiency of diagnosis. There are three main categories of fault diagnosis methods for power electronic circuits: analytical model-based, signal processing-based, and knowledge-based. Among them, the knowledge-based artificial neural network fault diagnosis method is the most commonly used method for diagnosing and analyzing power electronic circuit faults [9], since it does not require the establishment of precise and complex mathematical models, nor does it need to discriminate the patterns of signals, and it also has the ability of self-learning and memory. In the actual design of artificial neural networks, a widely used network model is the BP network and its variations, which has a non-linear mapping property that can be used to diagnose faults in rectifiers. The process is as follows: a sample of the fault waveform is input into the neural network and then trained to memorize the fault waveform. When a fault waveform within the diagnostic range is input into the trained neural network, the neural network will automatically diagnose the location of the faulty thyristor.

Since the BP network-based fault diagnosis has problems such as slow convergence and the tendency to converge to local minima, it needs to be optimized in conjunction with other intelligent optimization algorithms. In [10], a prediction algorithm using the Modified Multi-Strategy Sparrow Search Algorithm (MSSA) to optimize BP networks is proposed. The weights and thresholds of the BP network are optimized to make up for the shortcomings of the traditional BP algorithm, which enhances the ability of optimized search and improves the speed and accuracy of convergence. In [11], an algorithm that uses a combination of an annealing algorithm (SA) and a genetic algorithm (GA) to optimize a neural network (SAGA-BP) is proposed. By combining the advantages of the two algorithms to optimize the initial weights and thresholds of the neural network, the ability to quickly jump out of the local optimum solution is improved and high-accuracy localization is achieved. In [12], an algorithm combining Improved Beetle Antenna Search (IBAS) and BP neural network is proposed. Experimental results show that the IBAS-BP model not only effectively avoids the possibility of local minima, but also has higher prediction accuracy and better robustness.

Based on the above analysis, an improved particle swarm optimization (IPSO) algorithm is proposed to optimize the backpropagation (BP) network for identifying various fault types of thyristors in three-phase rectifier circuits, using a three-phase rectifier circuit as an example. The experimental results show that this method is simple, intuitive, and has high fault diagnosis accuracy.

2 Thyristor fault analysis in three-phase rectifier circuits

The three-phase rectifier circuit consists of six thyristors and a resistive load with the structure shown in Fig. 1. These six thyristors conduct in sequence from VT1 to VT6.

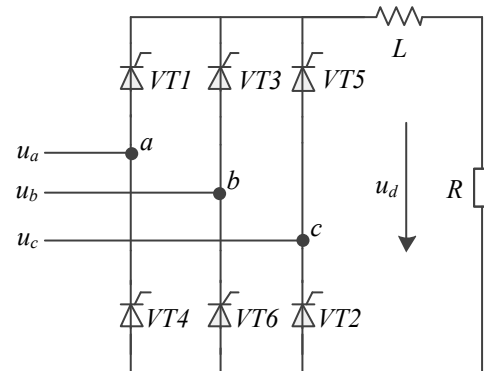


Fig. 1. Structure diagram of a three-phase rectifier circuit.

Open-circuit fault is one of the common faults in rectifier circuits, and this paper categorizes the open-circuit faults into the following five types: Type I, no thyristor damage; Type II, only one thyristor damage; Type III, two thyristors of the same phase voltage damaged at the same time; Type IV, two thyristors on the same half of the bridge damaged at the same time; and Type V, two thyristors of the cross damaged at the same time.

In this paper, the output voltage U_d at the load terminal is selected as the object of diagnostic analysis. In Simulink software, the circuit in Figure 1 is modeled and simulated, and the waveform of U_d can be obtained under the trigger angle $\alpha=0^\circ$, as shown in Figure 2, which is characterized by: the u_d waveforms under different major types of faults are very different; and under the faults of the same major type and different sources of faults, the shape of the u_d waveforms is unchanged, only shifted on the time axis. When α changes, the u_d waveform also changes. Images a to h are all from Figure 2

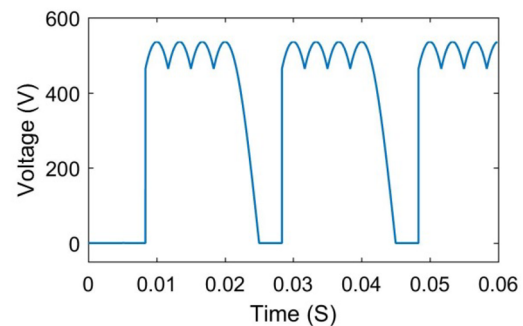


Fig. a. Fault voltage of VT1.

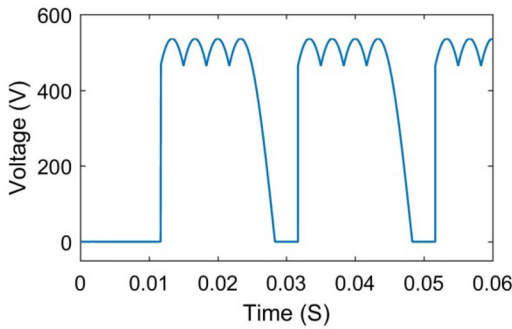


Fig. b. Fault voltage of VT2.

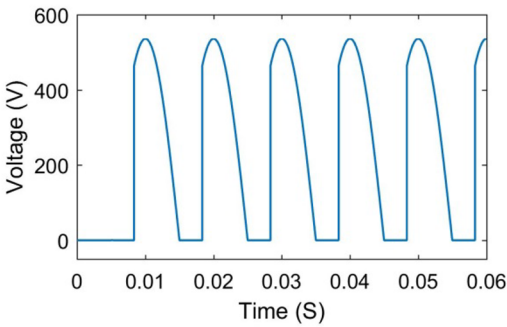


Fig. c. Fault voltage of VT1 and VT4.



Fig. d. Fault voltage of VT3 and VT6.

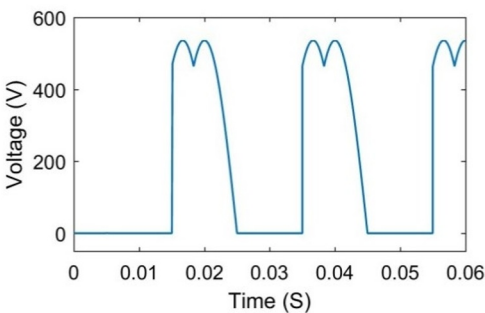


Fig. e. Fault voltage of VT1 and VT3.

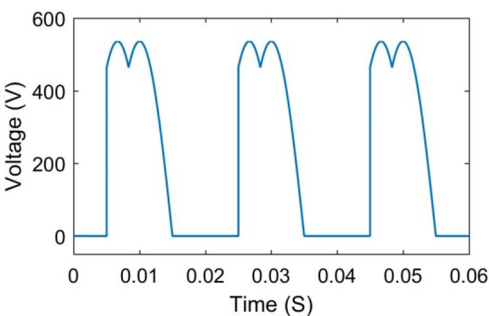


Fig. f. Fault voltage of VT4 and VT6.

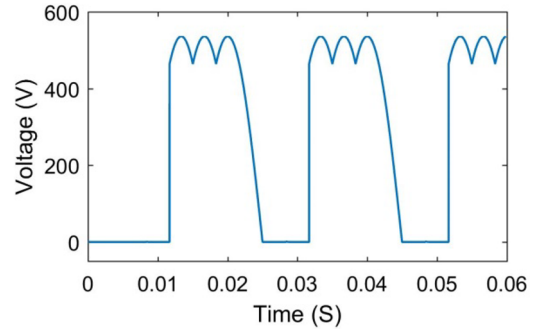


Fig. g. Fault voltage of VT1 and VT2.

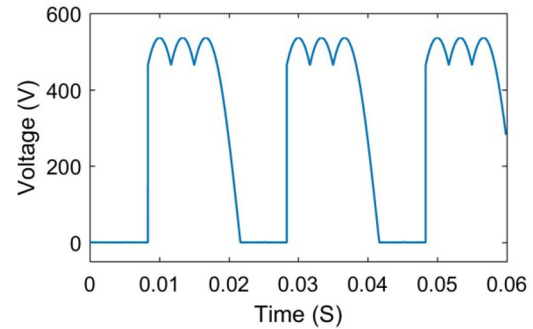


Fig. h. Fault voltage of VT1 and VT6.

Fig. 2. Output voltage waveform for type 4 faults ($\alpha = 0^\circ$).

Through analysis of the simulation diagrams for all fault types, it can be seen that for the same broad type of fault and different fault sources, although the shape of the u_d waveform is similar, the timing of the output voltage peak at the same cycle is different. Therefore, in this paper, we take the fifth type of fault as an example. The fault characteristic information is selected as the time of the peak output voltage in the same cycle, and the BP network is used to make judgments on specific thyristor faults. The following are stipulated here: the category label for VT1 and VT6 faults is 1; the category label for VT1 and VT2 faults is 2; the category label for VT2 and VT3 faults is 3; the category label for VT3 and VT4 faults is 4; the category label for VT4 and VT5 faults is 5; and the category label for VT5 and VT6 faults is 6.

3 Algorithm for optimizing BP neural networks using IPSO Algorithm

3.1 BP network algorithm

BP networks consist of multilayer networks, which are one of the most widely used neural network models [16]. When a BP network is used for fault diagnosis, it only needs to be provided with a large amount of data with input-output mapping relationships to complete the diagnosis, and no specific mathematical model is required. The fault diagnosis model of the BP network consists of three main layers: The input layer, which imports various fault information; The hidden layer, which processes the fault information obtained from the input layer and transmits it to the output layer by forward propagation; The output layer, which iteratively adjusts the coefficients of the network by a backpropagation algorithm according to the generated

errors and classifies the input according to the defined patterns [17]. The structure of the BP network is shown in Figure 3.

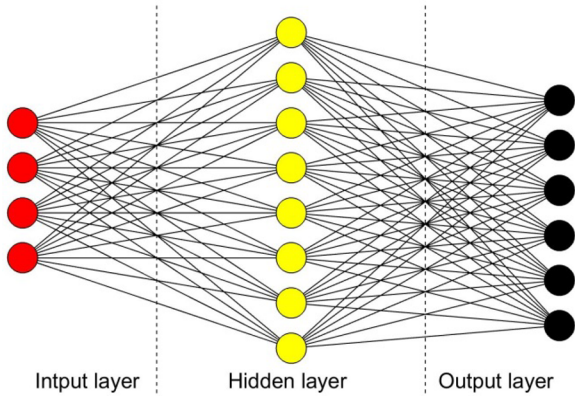


Fig. 3. The structure of a BP network.

The hidden layer activation function of a BP network is a combinatorial function with quadratic properties. The function is continuously differentiable and is usually described with a Sigmoid function:

$$O^{(r)}_{i,k,n} = \frac{1}{1 + \exp(-n^{(r)}_{i,k,n})} \quad (1)$$

Where $n^{(r)}_{i,k,n}$ represents the total input of the nodes in the previous layer; $O^{(r)}_{i,k,n}$ represents the output of the nodes. The operation process of the BP network is mainly divided into a training stage and a testing stage. In the training stage, the neural network is allowed to learn through various training samples, and the difference between the expected value and the actual value is used to repeatedly modify the connection weights of each neuron until the output of the network meets the requirements; In the testing stage, test samples are input into the trained network to classify various faults, which is used to test the effectiveness of the network training.

3.2 IPSO Algorithm

In this paper, an improved particle swarm optimization (IPSO) algorithm is used to optimize the BP network. The basic idea of particle swarm optimization of the BP network is that the initial connection weights of the BP network are regarded as a particle, and the particle swarm algorithm is used to globally optimize the initial connection weights of the network. In the particle swarm algorithm, assuming that the search space of the objective is D-dimensional, the potential optimal solution of each extreme value optimization problem is a particle in the space, and the fitness value of each particle is computed by its objective function, which evaluates the performance of the particle [15].

In the search for the optimal solution, the particle keeps track of two extremes: a locally optimal solution found by the particle itself, and a globally optimal solution found by the whole population. The two extremes are used by the particle to update its position and velocity in real time. Assuming the population size is N, the number of iterations is k. The formula for the position and velocity updated for the *i*th particle is

$$x^{k+1}_{iD} = x^k_{iD} + v^{k+1}_{iD} \quad (2)$$

$$v^{k+1}_{iD} = \omega v^k_{iD} + c_1 r_1 (p^k_{iD} - x^k_{iD}) + c_2 r_2 (p^k_{gD} - x^k_{iD}) \quad (3)$$

where ω is the inertia weight; c_1 and c_2 are acceleration factors; r_1 and r_2 are the random numbers of [0,1]; p_{kiD} is the current individual extremum of the particle; p_{kgD} is the current global extremum of the population; v_{kiD} and x_{kiD} are the velocity and position of the particle respectively.

The inertia weight ω is a very important parameter in the PSO algorithm, which is used to control the inertia of the particle search flight and directly affects the strength of the algorithm's search capability. The practical study shows that if ω can be changed adaptively as the optimization proceeds, then the PSO algorithm will be able to balance the global search capability and the local search capability at different stages of the evolution. In this paper, the adaptive change of inertia weights is achieved by using a linear control strategy. In the early stage of the search, the value of ω is larger, and the global search ability of the particle is enhanced to avoid falling into the local optimum; in the process of the search, the value of ω decreases linearly, and the ability of the local search is gradually enhanced; in the late stage of the search, the value of ω is smaller, which focuses on the detailed search, and the global optimum solution is precisely determined. The formula for the inertia weights is

$$\omega = \omega_{\max} - (\omega_{\max} - \omega_{\min}) * k / k_{\max} \quad (4)$$

Where ω_{\min} and ω_{\max} denote the minimum and maximum values of inertia weights, respectively. In this paper, the performance of the PSO algorithm reaches the best effect when $\omega_{\min} = 0.4$ and $\omega_{\max} = 0.8$ are selected. The particle also has to determine whether it exceeds the set boundary range after each update of its velocity and position. If it exceeds, this paper directly constrains it to the boundary and replaces the current value with the boundary value. Because each particle also influences inertia and learning factors, even if the constraint is back to the boundary, it will be an optimization search again. The PSO algorithm is a global optimization strategy, the algorithm is simple, the global search ability is strong, and the combination with the BP neural network can improve the convergence speed of the learning process to avoid falling into the local minima.

4 Experiment results and discussion

4.1 Fault classification for BP networks

All fault types at trigger angles $\alpha=0^\circ$, 30° , and 60° are selected as training samples, and the number of training samples is 18. All fault types at $\alpha=90^\circ$ are selected as test samples, and the number of test samples is 6. The structure of the BP network is set as 3 layers, 3 input nodes, 8 hidden layer nodes, and 1 output node. The results of fault classification based on the BP network are shown in Fig. 4. From Fig. 4, we know that the training data classification results are consistent with the target results, so the training effect of the BP network is good. The test data classification results have a certain

deviation from the target results and do not completely fit the actual values.

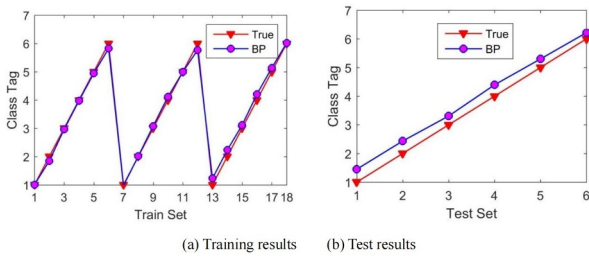


Fig. 4. Classification results of BP network

4.2 IPSO algorithm optimization of BP networks for fault classification

By IPSO algorithm to optimize the parameters of the BP network, diagnostic accuracy can be improved. The initial population of PSO is set to 100, and the two acceleration factors are set to 2. The effect of PSO optimization of the BP network is shown in Fig. 5, the comparisons of epochs are shown in Fig.6, and the error comparison effect graphs of the test are shown in Fig. 7. From Fig. 5, it can be seen that the PSO-BP network is consistent with the target results for the classification of training data, so the training effect is good. From Fig. 6 and Fig. 7, it can be seen that the BP network optimized by PSO algorithm predicts the obtained classification results closer to the target results, with smaller error and shorter time compared to the BP network, and the troubleshooting accuracy and diagnosis and time of the network are greatly improved, which achieves the expected results.

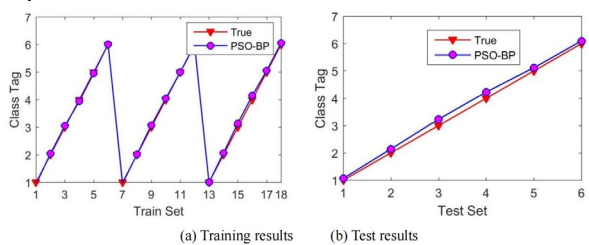


Fig. 5. PSO-BP network classification results

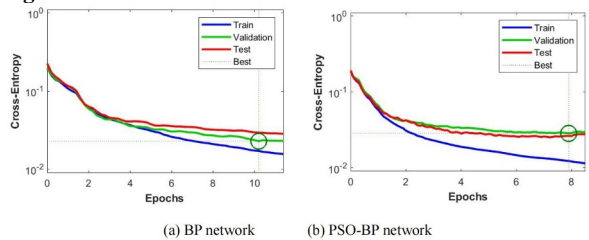


Fig. 6. Comparison of epochs

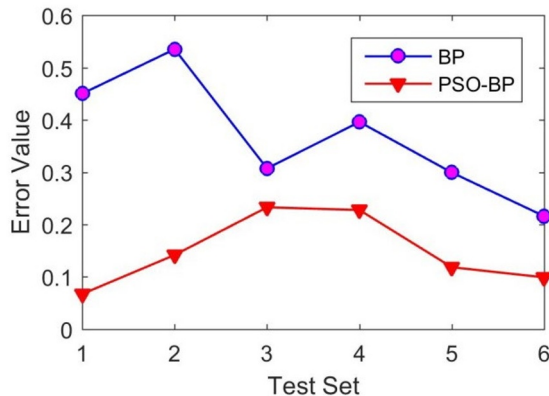


Fig. 7. Comparative effect of test errors

5 Conclusion

This paper proposes an IPSO algorithm to optimize BP networks for fault diagnosis of three-phase rectifier circuits. Through the analysis of the fifth category of faults in the three-phase rectifier circuit, the time of the peak output voltage of the same cycle is extracted as a feature sample, normalized, and input to the BP, improved PSO-BP algorithm for fault diagnosis. The simulation experiment results show that the test classification results of the algorithm match the target results and achieve good results. This effectively solves the problem of determining which thyristor is damaged due to similar output voltage waveforms in the same fault type, and the reliability and accuracy of fault diagnosis for three-phase rectifier circuits have been improved. The algorithm can be extended to the fault diagnosis of other power electronic circuits.

Funding Statement: This work was supported by the 2024 Project for Improving the Basic Research Ability of Young and Middle-aged Teachers in Guangxi Universities (Grant No. 2024KY0232).

References

1. B. Song, C. Kang, L. Xu and J. Zhang, "Fault Diagnosis of Three-phase Full-bridge Rectifier Circuit based on Deep Neural Network," 2018 Chinese Automation Congress (CAC), Xi'an, China, 2018, pp. 468-473, doi: 10.1109/CAC.2018.8623247.
2. B. Li, S. Shi, B. Wang, G. Wang, W. Wang and D. Xu, "Fault Diagnosis and Tolerant Control of Single IGBT Open-Circuit Failure in Modular Multilevel Converters," in IEEE Transactions on Power Electronics, vol. 31, no. 4, pp. 3165-3176, April 2016, doi: 10.1109/TPEL.2015.2454534.
3. F. Wu and J. Zhao, "Current Similarity Analysis-Based Open-Circuit Fault Diagnosis for Two-Level Three-Phase PWM Rectifier," in IEEE Transactions on Power Electronics, vol. 32, no. 5, pp. 3935-3945, May 2017, doi: 10.1109/TPEL.2016.2587339.
4. G. Zhang and J. Yu, "Open-circuit fault diagnosis for cascaded H-bridge multilevel inverter based on LS-PWM technique," in CPSS Transactions on Power Electronics and Applications, vol. 6, no. 3, pp. 201-208, Sept. 2021, doi: 10.24295/CPSS/TEA.2021.00018.
5. M. Chen and Y. He, "Open-Circuit Fault Diagnosis Method in NPC Rectifiers Using Fault-Assumed Strategy," in IEEE Transactions on Power Electronics, vol. 37, no. 11, pp. 13668-13683, Nov. 2022, doi: 10.1109/TPEL.2022.3183075.
6. K. Zhang, B. Gou and X. Feng, "Online Fault Diagnosis for Single-Phase PWM Rectifier Using Data-Driven Method," in CPSS Transactions on Power Electronics and Applications, vol. 7, no. 1,

pp. 49-57, March 2022, doi:

[10.24295/CPSSTPEA.2022.00005](https://doi.org/10.24295/CPSSTPEA.2022.00005).

7. A. Z. Nejad and A. Dastfan, "Fault detection and reconfiguration of the 12-pulse thyristor rectifier," *2023 10th Iranian Conference on Renewable Energy & Distributed Generation (ICREDG)*, Shahrood, Iran, Islamic Republic of, 2023, pp. 1-7, doi: [10.1109/ICREDG58341.2023.10092138](https://doi.org/10.1109/ICREDG58341.2023.10092138).
8. Z. Wang, Y. Li and X. Yin, "Visual MMC Open Circuit Fault Real-Time Rapid Detection System," in *IEEE Access*, vol. 11, pp. 15030-15037, 2023, doi: [10.1109/ACCESS.2023.3243832](https://doi.org/10.1109/ACCESS.2023.3243832).
9. R. Aljarrah et al., "Application of Artificial Neural Network-Based Tool for Short Circuit Currents Estimation in Power Systems With High Penetration of Power Electronics-Based Renewables," in *IEEE Access*, vol. 11, pp. 20051-20062, 2023, doi: [10.1109/ACCESS.2023.3249296](https://doi.org/10.1109/ACCESS.2023.3249296).
10. X. Tang, D. Feng, K. Li, J. Liu, J. Song et al., "An improved bpsn prediction method based on multi-strategy sparrow search algorithm," *Computers, Materials & Continua*, vol. 74, no.2, pp. 2789–2802, 2023.
11. W. Wang, Q. Zhu, Z. Wang, X. Zhao and Y. Yang, "Research on Indoor Positioning Algorithm Based on SAGA-BP Neural Network," in *IEEE Sensors Journal*, vol. 22, no. 4, pp. 3736-3744, 15 Feb.15, 2022, doi: [10.1109/JSEN.2021.3120882](https://doi.org/10.1109/JSEN.2021.3120882).
12. Z. Liu, Q. Tan, Y. Zhou and H. Xu, "Syncretic Application of IBAS-BP Algorithm for Monitoring Equipment Online in Power System," in *IEEE Access*, vol. 9, pp. 21769-21776, 2021, doi: [10.1109/ACCESS.2021.3055247](https://doi.org/10.1109/ACCESS.2021.3055247).
13. R. Zhang, Z. -B. Xu, G. -B. Huang and D. Wang, "Global Convergence of Online BP Training With Dynamic Learning Rate," in *IEEE Transactions on Neural Networks and Learning Systems*, vol. 23, no. 2, pp. 330-341, Feb. 2012, doi: [10.1109/TNNLS.2011.2178315](https://doi.org/10.1109/TNNLS.2011.2178315).
14. X. Pan, W. Zhou, Y. Lu and N. Sun, "Prediction of Network Traffic of Smart Cities Based on DE-BP Neural Network," in *IEEE Access*, vol. 7, pp. 55807-55816, 2019, doi: [10.1109/ACCESS.2019.2913017](https://doi.org/10.1109/ACCESS.2019.2913017).
15. S. Mahapatra, M. Badi and S. Raj, "Implementation of PSO, it's variants and Hybrid GWO-PSO for improving Reactive Power Planning," *2019 Global Conference for Advancement in Technology (GCAT)*, Bangalore, India, 2019, pp. 1-6, doi: [10.1109/GCAT47503.2019.8978348](https://doi.org/10.1109/GCAT47503.2019.8978348).